Electrochemical Hydrogen Pump using a High Temperature Type Proton Conductor under Reduced Pressure

Masahiro TANAKA

National Institute for Fusion Science, Oroshi, Toki, Gifu, 509-5292, Japan

The electrochemical hydrogen pump properties of the $CaZr_{0.9}In_{0.1}O_{3-\alpha}$ proton conductor were observed under reduced pressure condition in the cathode compartment for the recovery of hydrogen isotopes. The applied voltage between electrodes under reduced pressure condition reduced than that under atmospheric pressure condition, when the hydrogen pump performance was evaluated by direct current method. It is likely that the total pressure in the cathode compartment affects the overall electric resistance. From the impedance spectroscopy analysis, it was suggested that diffusion process in porous electrode was affected by reduced pressure condition. The hydrogen pump performance could be improved under the reduced pressure condition of around few kPa and the reduced pressure condition had an effect on the mass transfer process in the electrode.

Keywords: proton conductor, hydrogen pump, tritium recovery, reduced pressure, electrochemical impedance spectroscopy, charge transfer process, mass transfer process.
.

1. Introduction

In a future nuclear fusion plant, hydrogen isotope gas of deuterium (D) and tritium (T) is used as fuel. The developments of hydrogen process technologies for fuel cycle are one of the important issues. As for the hydrogen isotope recovery process for chemical purification of hydrogen, the candidate material is a palladium membrane diffuser [1]. Hydrogen permeates through the membrane by providing pressure difference as a driving force and high purity hydrogen gas is obtained. However, the palladium membrane cannot directly recovery hydrogen in the hydrogen compounds such as water vapor and hydrocarbons. Thus, it has been suggested to decompose hydrogen compounds to hydrogen gas by a cracking catalysts or electrochemical reactor, and the membrane reactor systems combined with cracking catalyst have been researched and developed [2-4].

An electrochemical hydrogen pump using a proton-conducting oxide is one of the candidate materials for hydrogen recovery. Some perovskite-type oxides such as $SrCeO_3$, $CaZrO_3$, and $SrZrO_3$ which are doped with Yb^{3+}, Y^{3+} and In^{3+} etc exhibit proton conduction in hydrogen-containing atmospheres at high temperature [5]. It has attractive advantages such as: hydrogen extraction from both hydrogen molecules and hydrogen compounds; control by electric current; no pressurization, etc. Thus, the application of electrochemical hydrogen pump by a proton conducting oxide instead of the palladium membrane diffuser have been proposed by Asakura [6] and Kawamura et al. [7,8]. In our previous research, we have

chosen $CaZr_{0.9}In_{0.1}O_{3-\alpha}$, which was used for the one-end closed tube of the test pump, as the proton-conducting oxide, because $CaZr_{0.9}In_{0.1}O_{3-\alpha}$ is excellent in the chemical stability against carbon dioxide attack at elevated temperature and in mechanical strength. Then, the hydrogen pump performances under various conditions have been reported and shown the possibility of realization [9,10]. On the other hands, in order to recovery pure hydrogen isotope gases for fuel cycle, hydrogen pump into a vacuum would be required to avoid from being mixed in impurity gaseous as purge gas. However, the hydrogen pump characteristics into vacuum are not well-known. Kato et al. have proposed a small tritium purification and recovery system for muon-catalyzed fusion (μCF) and have evaluated hydrogen pump performance using a high temperature type proton conductor under a high vacuum condition [11]. As the results, although they showed that hydrogen could be extracted into vacuum, the dependence of total pressure in the cathode compartment has not been studied in detail.

As to the applications of proton conductor in vacuum technology, Schober has demonstrated a novel water vapor and hydrogen gas source into vacuum, and then proposed as a leak detector for vacuum purposes [12, 13]. These reports, however, were also not considered the dependence of total pressure in the cathode compartment on hydrogen pump.

In this research, we report the preliminary results of the hydrogen pump characteristics under reduced pressure condition in the pressure range from 10 Pa to 10^5 Pa.
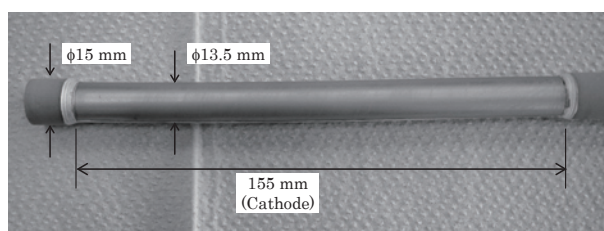
author's e-mail: tanaka.masahiro@nifs.ac.jp

Fig.1 A photograph of one end closed proton conductor; $CaZr_{0.9}In_{0.1}O_{3-\alpha}$.

2. Experimental
2.1 Proton Conducting Oxide

From the viewpoint of the practical use, we carried out the performance tests by use of the one end closed tube made of $CaZr_{0.9}In_{0.1}O_{3-\alpha}$, which was prepared by TYK Co. Ltd. The shape of the test tube was 12 mm inner diameter, 0.75 mm thickness and 340 mm length. The appearance of test tube is shown in Fig. 1. Platinum electrodes were attached on both sides of the test tube by paste-baking on
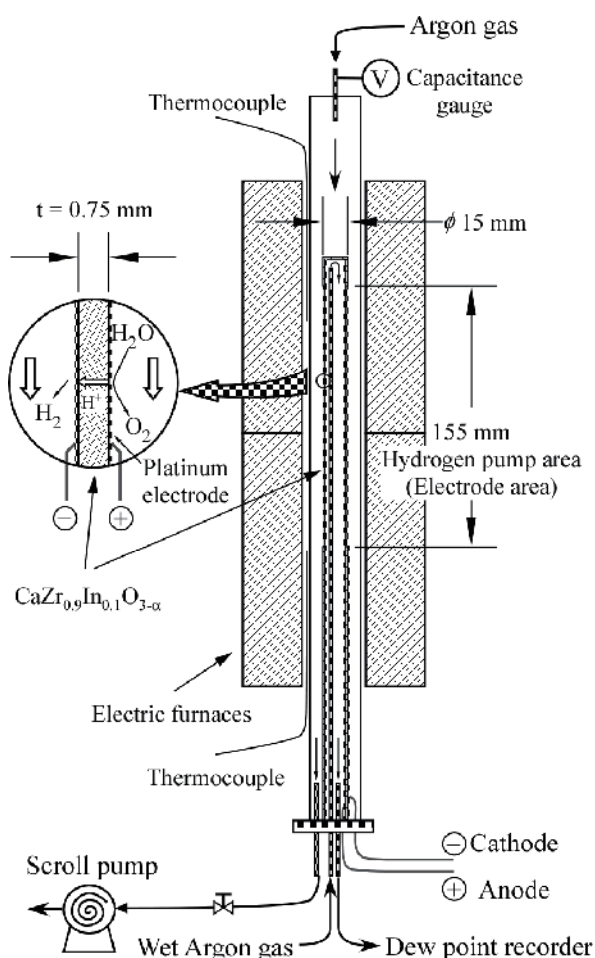

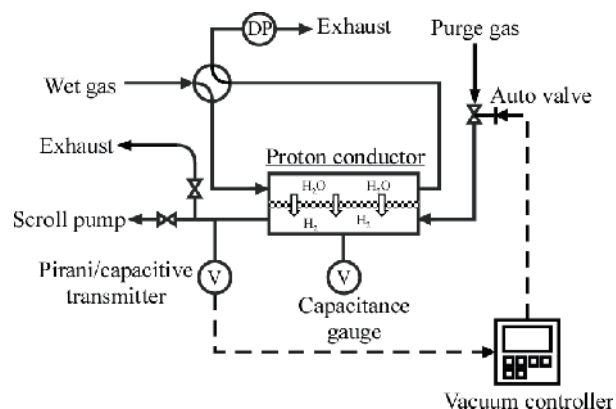Fig.2 Schematic of the hydrogen pump apparatus.

Fig.3 Flow diagram of hydrogen pump apparatus and vacuum control system.

the inner surface. The electrode on the outer surface was attached by electroless-plating method. The each electrode of inner and outer surfaces was used as anode and cathode, respectively. In addition, a platinum paste 5 mm in width as a collector electrode was also calcined from top to bottom on the outer surface. The effective electrode length along the axial direction at the outer surface was about 155 mm and that at the inner surface was 340 mm. The effective outer electrode was approximately 62 cm^2.

2.2 Hydrogen Pump Apparatus and Vacuum Control System

Schematic diagrams of the hydrogen pump apparatus and the vacuum control system are shown in Fig. 2 and 3. The test tube was heated from 873 K to 1073 K by an electric furnace. The gas was humidified by using a bubbler immersed in a constant-temperature water bath controlled at 283K. Wet argon gas was fed to the anode side at 100 cm^3/min and the flow rate was controlled by a mass flow controller. The electrochemical hydrogen pump through the specimens was examined by sending direct current with a potentio/galvanostat (HOKUTO DENKO, HA-151) to the following electrolytic cell:

$$(+)\ Ar+H_2O,\ Pt/CaZr_{0.9}In_{0.1}O_{3-\alpha}/Pt,\ Ar\ (-),\qquad (1)$$

The accuracy of the voltage measurement was ± 3 mV. An impedance analysis measurement was conducted by use of two LCR meters with different frequency range (HIOKI, 3522-50 and 3532-80). These frequency ranges are 1 mHz to 100 kHz and 4 Hz to 1 MHz, respectively. The pressure in the cathode was measured by a capacitance vacuum gauge (MKS, Baratoron 626A) in the measuring pressure range of 10 Pa to 10^5 Pa.

In this experimental system, the total pressure in the cathode compartment could be reduced until around 10 Pa by a scroll type vacuum pump (Sato Vacuum Inc, OFS-M-300). Then, the pressure in the cathode

compartment was up to 10^5 Pa by introducing argon gas. The pressure was controlled by a gas dosing system control unit (Pfeiffer vacuum, RVC-300 and RME 005 valve) with a pirani/capacitive transmitter (Pfeiffer vacuum, PCR-260). The dew point was measured with a chilled-mirror dew point recorder (General eastern, 1311DR). The accuracy of dew point measurement is ±0.2 ^{o}C.

3. Experimental Results and Discussion

3.1 Hydrogen Pump Characteristics under Reduced Pressure

Figure 4 shows the dependence of voltage on total pressure in the cathode compartment for different current density at 973K. Each pressure condition was maintained for about 10 minutes. As seen in the figure, a very small change of voltage was observed with variation of total pressure. All the voltage value under reduced pressure was smaller than the voltage of atmospheric pressure in spite of current density. The voltage was minimized around 10 kPa and the voltage drop was the range of 0.04 V to 0.07 V each current density. It is probable that the appearance electric resistance decreased slightly under reduced pressure condition. However, the voltage slightly increased under reduced pressure less than 1 kPa. It is likely that the total pressure in the cathode compartment affects the overall electric resistance.

The dew point at anode compartment decreased with increase of current density. However, the dependency of dew point on the total pressure at the cathode compartment was not observed clearly due to the resolution of the dew point recorder. Therefore, it was not clear whether
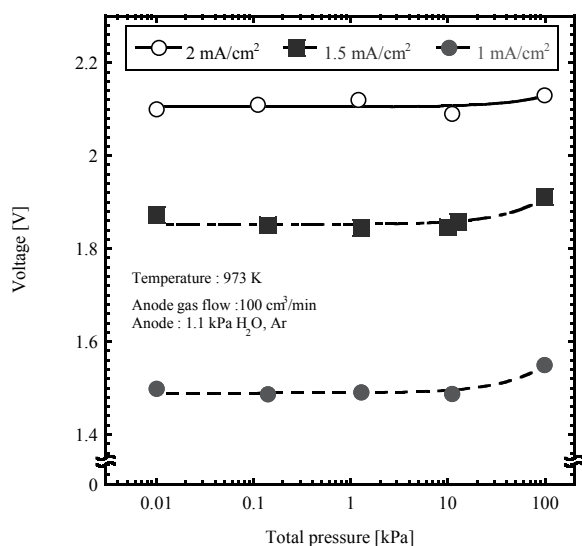

Fig.5 Current-voltage relationship on different total pressure condition in the cathode compartment.

Fig.4 Dependence of voltage on total pressure in the cathode compartment for different current density at 973K.

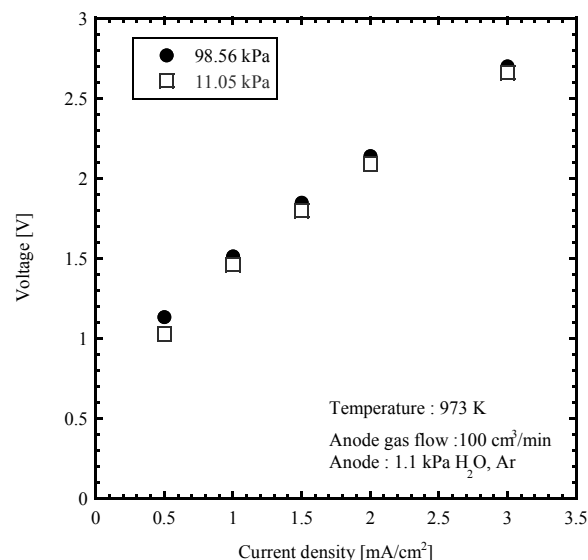hydrogen evolution rate under reduced pressure condition was enhanced or not.

Figure 5 shows the relationship between current density and voltage under the different total pressure condition of 11.05 kPa and 98.56 kPa in the cathode compartment at 973 K. The voltage at 11.05 kPa was lower than that at 98.56 kPa. Although the voltage of each pressure condition increased with increase of current density, the difference in voltage between 11.05 kPa and 98.56 kPa decreased with increasing current density. When current density increases, more hydrogen gas is extracted to the cathode electrode. From the viewpoint of the mass transfer process, the mass transfer resistance would mainly consist of three phenomena: proton migration in the electrolyte, the electrode reaction on both the anode and the cathode and gas diffusion in the porous electrode. The gas diffusion in the porous electrode would be affected by both the porous diameter of electrode and mean free path. If the pore diameter of the electrode is larger than the mean free path which is the function of the reciprocal of gas pressure, the diffusion phenomenon is considered bulk diffusion. On the other hands, when the pore diameter of the electrode is less than the mean free path, the diffusion phenomenon is close to Knudsen diffusion. It is not clear that ether pore diffusion effects can be applied, because the hydrogen partial pressure in the pore electrode and the pore diameter of electrode are not determined with accuracy. These gas diffusion phenomena in the porous electrode are appeared as electrochemical polarization and the impedance would be increased. Then, to separate the mass transfer phenomena, the impedance spectroscopy analysis was carried out in the next section.

3.2. Impedance Spectroscopy Analysis

Impedances spectroscopy analysis is powerful method of characterizing of the electrical properties of materials and the interface of electrode [14]. It may be used to analysis the charge and mass transfer processes [15]. In this report, we discuss qualitatively the impedance behavior using a simple model incorporated the charge and mass transfer processes as the first step.

3.2.1. Electrochemical Impedance Spectroscopy

Electrochemical impedance spectroscopy is a technique for characterization of electrochemical system. In general, an electrochemical cell can be considered simply impedance circuit to a small sinusoidal excitation; hence the electrochemical cell is able to be represented by an equivalent circuit of resistors, capacitors, inductor, constant phase element and impedance as a model of diffusion at the electrode interface, etc. These elements are combined with series and/or parallel to make complex equivalent circuit. A simple and common use semi-empirical model for an electrochemical cell is the Randles circuit which describes the response of a single-step charge-transfer process with diffusion [14, 16]. It consists of an electrolyte resistance R_s in series with the parallel combination of the double-layer capacitance C_{dl} and the charge transfer resistance R_{ct} and the combined impedance Z is expressed as follow:

$$Z = R_S + \frac{R_{ct}}{j\omega R_{ct}C_{dl} + 1}, \qquad (2)$$

These elements are modified depending on the charge transfer and mass transfer processes such as chemical reaction, gas diffusion and adsorption etc. Taking into consideration of the elementary processes in/on proton conductor, the faraday impedance Z_F, which is due to chemical process, mass transfer process and adsorption process etc around the electrode, instead of the charge transfer impedance R_{ct} may be applied as the diffusion impedance. The Z_F with finite-length diffusion impedance is expressed by following equation [14, 17]:

$$Z_F = R_{ct} + \frac{K}{\sqrt{j\omega D}}\tanh\left[-\delta\sqrt{\frac{j\omega}{D}}\right]$$
$$= R_{ct} + Z_{D,} \qquad (3)$$

where, j is imaginary unit, ω is angular frequency, K is constant of diffusion impedance, D is effective diffusivity of gas through porous layer, δ is diffusion distance. The first and second terms express the charge transfer resistance R_{ct} and the diffusion impedance Z_D, respectively. The limiting value of Z_F under high and low frequency are express as follows:
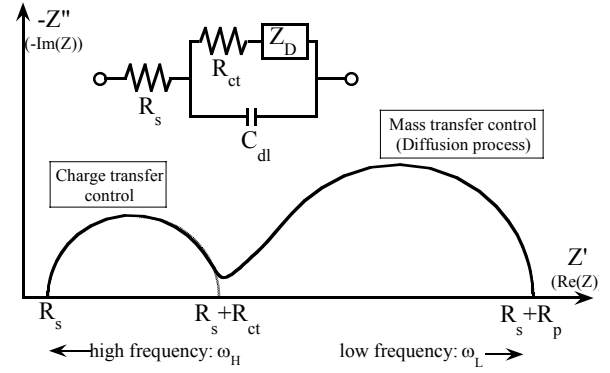

Fig.6 Illustrating of the impedance spectrum of the Randles circuit with the faraday impedance of finite-length diffusion.

$$Z_{F,\omega\to\infty} = R_{ct}, \qquad (4)$$

$$Z_{F,\omega\to0} = R_{ct} + \frac{K\delta}{D} = R_p, \qquad (5)$$

where, R_p is polarization resistance. To identify and separate the different processes, it is useful to represent the measured impedance spectra as Nyquist plot. Figure 6 shows a calculated illustration of the impedance spectrum of the Randles circuit with faraday impedance as Nyquist plot. The impedance spectrum has two semicircles. The left semicircle, which is high frequency region, corresponds to the parallel circuit of C_{dl} and R_{ct} and represents the charge transfer process. The right semicircle corresponding to low frequency region represents the impedance spectrum of faraday impedance of Eq. (3) as diffusion process. The shape of right semicircle depends on several parameters of gas effective diffusion coefficient D, constant K and diffusion distance δ.

In the experimental system, the compartments of the anode and the cathode have different conditions such as atmosphere, the electrode area and porosity. For the application of impedance analysis, these complicated effects should be taken into consideration. Therefore, in a general way, more complex equivalent circuits corresponding to the equivalent circuits of both conditions of anode and cathode than the simple Randle circuit as shown in Fig. 6 would be required to simulate the impedance spectrum. The impedance related to the diffusion is usually found in the lowest frequency range, down to 10 mHz or even lower [14]. Therefore, in the present study, since the operational parameter is only total pressure in the cathode compartment, the diffusion process in the cathode electrode would be discussed qualitatively from the experimental results of the impedance spectrum in next section.
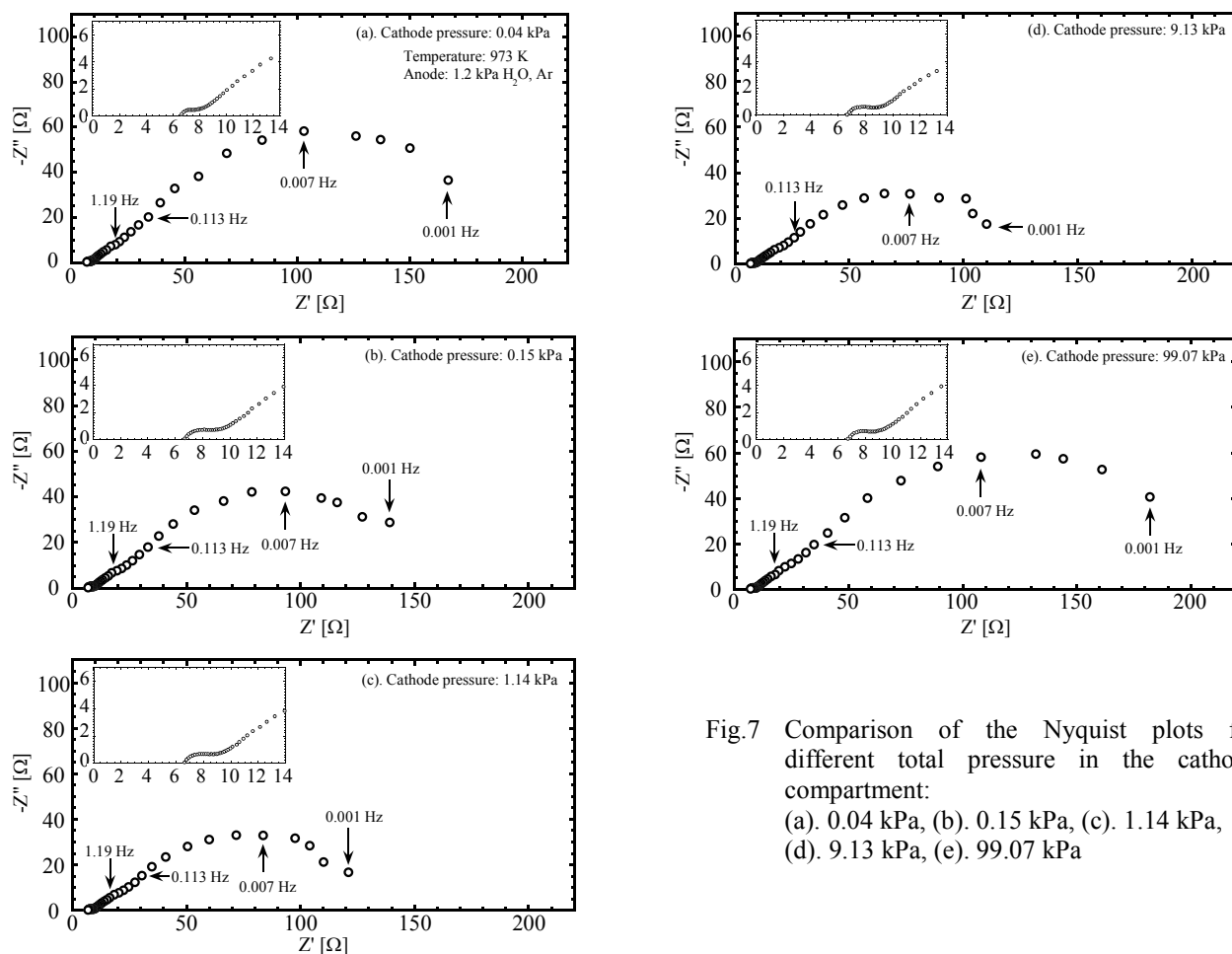
Fig.7   Comparison of the Nyquist plots for different total pressure in the cathode compartment:
(a). 0.04 kPa, (b). 0.15 kPa, (c). 1.14 kPa,
(d). 9.13 kPa, (e). 99.07 kPa

3.2.2. Impedance Behavior under Reduced Pressure Condition

Figure 7 shows comparison of the Nyquist plots for different total pressure in the cathode compartment at 973 K. The Nyquist plots of lower impedance region measured by LCR meter 3532-80 were shown in the higher left hand corner of each figure. It seems that the impedance spectra of this system had two or three semicircles. The left semicircle seems not to be almost affected the total pressure variations in the cathode compartment, while the shape of right semicircle is much changed by the variation of total pressure. As shown in Fig. 6, the left semicircle would represent the charge transfer control in the electrolyte-electrode interface and the left endpoint of semicircle corresponds to electrolyte resistance. Therefore, the left semicircle would be almost independent of the total pressure.

On the other hand, the right semicircle would represent the mass transfer control with diffusion process of faraday impedance, Z_F. According to Eq. (3) and (5), the semicircle of diffusion process should become smaller with decreasing total pressure until few kPa, because the pressure dependence of diffusivity of gas is correlated to

P^{-1} according to the Chapman-Enskog theory [18]. However, the semicircle became larger at the total pressure below 1 kPa. The pressure dependence of impedance spectra is corresponding to that of the voltage variations on hydrogen pump as shown in Fig. 4. The diffusion effects as described in section 3.1 might be being shifted depending on the total pressure below 1 kPa. Although the mechanism of the increase in the impedance spectra less than 1 kPa could not be determined in this report, it might be suggested that the hydrogen pump performance could be improved under the reduced pressure condition of around few kPa and the reduced pressure condition has an effect on the mass transfer process in the electrode.

4. Conclusion

The electrochemical hydrogen pump properties of the $CaZr_{0.9}In_{0.1}O_{3-\alpha}$ were observed under reduced pressure condition in the cathode compartment. From the behavior of hydrogen pumping under reduced pressure atmosphere, it is suggested that the total pressure in the cathode compartment affects the overall electric resistance. From the impedance spectroscopy analysis, it was suggested that diffusion process in porous electrode was affected by

reduced pressure condition. It might be suggested that the hydrogen pump performance could be improved under the reduced pressure condition of around few kPa and the reduced pressure condition had an effect on the mass transfer process in the electrode.

Acknowledgements

[1]   H. Yoshida *et al.*, Nucl. Technol. Fusion, **3**, 471 (1983).
[2]   S.A. Birdsell *et al.*, Fusion Technol., **30**, 905 (1996).
[3]   B. Bornschein *et al.*, Fusion Sci. Technol., **48**, 11 (2005).
[4]   S. Konishi *et al.*, Fusion Technol., **30**, 890 (1996).
[5]   H. Iwahara *et al.*, Solid State Ionics, **168**, 299 (2004).
[6]   Y. Asakura, J. Plasma Fusion Res., **78**, 1319 (2002), [in Japanese].
[7]   Y. Kawamura *et al*, Fusion Eng. Des., **82**, 113 (2007).
[8]   Y. Kawamura *et al.*, Fusion Eng. Des., **83**, 625 (2008).
[9]   M. Tanaka *et al*., J. Nucl. Sci. Technol., **41**, 61 (2004).
[10]   M. Tanaka *et al.*, Fusion Eng. Des., **83**, 1414 (2008).
[11]   M. Kato *et al.*, Fusion Sci. Technol., **41**, 859 (2002).
[12]   T. Schober, Solid State Ionics, **144**, 379 (2001).
[13]   T. Schober and P. Meuffels, J. Vac. Sci. Technol., A **19**, 958 (2001).
[14]   E. Barsoukov and J.R. Macdonald ed., *Impedance Spectroscopy; Theory, Experiment, and Applications, second edition* (John Wiley & Sons, 2005), p. 497.
[15]   S. Fukada *et al*., J. Nucl. Sci. Technol., **42**, 305 (2005).
[16]   M.A. Danzer and E.P. Hofer, J. Power Sources, **190**, 25 (2009).
[17]   M. Itagaki, *Denkikagaku impedance hou* (Maruzen, 2008), p. 119, [in Japanese].
[18]   E.L. Cussler, *Diffusion: mass transfer in fluid system, third edition* (Cambridge University Press, 2009), p.119.